

A physically meaningful relationship between R50% and PTV surface area in lung SBRT

Dharmin D. Desai¹ | Ivan L. Cordrey^{1,*} | E. L. Johnson²

¹Radiation Oncology, CHI Memorial Hospital, Chattanooga, TN, USA

²Department of Radiation Medicine, University of Kentucky Chandler Medical Center, Lexington, KY, USA

Author to whom correspondence should be addressed. Ivan L. Cordrey
E-mail: Ivan-Cordrey@charter.net.

Abstract

Purpose: We propose a novel understanding of two characteristics of the planning target volume (PTV) that affect the intermediate-dose spill in lung stereotactic body radiation therapy (SBRT) as measured by R50%. This phantom model research investigates two characteristics of the PTV that have a marked effect on the value of R50%: the mean dose deposited within the PTV (D_{av}) and the surface area of the PTV (SA_{PTV}).

Methods: Using a phantom model provided by a CT of the IROC Thorax-Lung Phantom[®] (IROC Houston QA Center, Houston, TX) and Eclipse[®] Treatment Planning System (Varian Medical Systems, Palo Alto, CA), we investigate the two characteristics for spherical and cylindrical PTVs. A total of 135 plans with tightly controlled PTV characteristics are employed. A lower bound for R50% ($R50\%_{min_{\Delta r}}$) is derived and clearly establishes a relationship between R50% and SA_{PTV} that has not been fully appreciated previously.

Results: The study of PTV D_{av} revealed a local minimum for R50% as a function of the PTV D_{av} at $D_{av} \approx 110\%$ of Rx dose. As PTV D_{av} increases above this local minimum, R50% increases; while for PTV D_{av} less than this local minimum, the R50% value also increases. The study of PTV surface area (SA_{PTV}) demonstrated that as the SA_{PTV} increases, the R50% increases if the PTV volume stays the same. The SA_{PTV} result is predicted by the theoretical investigation that yields the R50% lower bound, $R50\%_{min_{\Delta r}}$.

Conclusions: This research has identified two characteristics of the PTV that have a marked influence on R50%: PTV D_{av} and SA_{PTV} . These characteristics have not been clearly articulated in the vast body of previous research in SBRT. These results could help explain plans that cannot meet the RTOG criteria for R50%. With further development, these concepts could be extended to provide additional guidance for creating acceptable SBRT plans.

KEY WORDS

lung, PTV mean dose, PTV surface area, R50%, R50% lower bound, SBRT

*Joint First Authorship: Desai and Cordrey should be considered joint first authors.

1 | INTRODUCTION

Stereotactic body radiation therapy (SBRT) was defined in 2014 as “a method of external beam radiotherapy (EBRT) that accurately delivers a high dose of irradiation in one or few treatment fractions to an extracranial target.”¹ This technique of high-precision, ultra-hypofractionated EBRT is gaining widespread clinical use facilitated by convenient, commercially available equipment that makes SBRT practical even in community-based radiation therapy facilities. Stereotactic body radiation therapy has been rapidly adopted as the standard of care for nonsurgical early-stage lung cancer.^{2–6}

The current clinical practice of SBRT for early-stage nonsurgical lung cancer treatment is based on the clinical protocols provided by three RTOG studies: RTOG 0236,⁷ RTOG 0813,⁸ and RTOG 0915.⁹ A principle metric for plan acceptability is R50%. R50% is a derived unitless quantity obtained from the volume of the 50% prescription isodose cloud (IDC50%) and the planning target volume (PTV) volume as follows:

$$R50\%(\text{unitless}) = \frac{\text{IDC50\% Volume}}{\text{PTV Volume}} \quad (1)$$

The IDC50% is a surrogate for damage to irradiated normal tissues as discussed in the work of Yang et al.¹⁰ The goal of SBRT treatment planning is to deliver a high dose to the target (for local tumor control) that meets or exceeds the minimum dose specified by the prescription while minimizing the IDC50% (to minimize normal tissue damage) and avoiding unacceptable dose to organs at risk (OAR).

The RTOG protocol⁹ provides guidance for acceptable values for R50% as function of the PTV volume measurement. Other RTOG-defined quantities used to assess SBRT plan quality are D2cm⁷ (maximum Dose 2 cm from the PTV in any direction), V105%⁹ (105% prescription isodose volume outside of the PTV), and CI⁹ (Conformity Index = [100% prescription Isodose Volume]/[PTV Volume]). In addition, these protocols contain limits on various OARs, such as the spinal cord and ribs.

When considering the PTV dose heterogeneity there are three metrics available: ICRU HI,⁹ RTOG HI,¹¹ and PTV mean dose (PTV D_{av}). The ICRU HI, RTOG HI, and PTV D_{av} are defined, respectively, as follows:

$$\text{ICRU HI} = \frac{(D_{2\%} - D_{98\%})}{D_{50\%}} \quad (2)$$

where D_{x%} = the minimum dose to x% of the PTV.

$$\text{RTOG HI} = \frac{D_{\max}}{D_{\text{Rx}}} \quad (3)$$

where D_{max} = “maximum dose in the PTV” and D_{Rx} = “prescription dose.”

And

$$\text{PTV } D_{\text{av}} = \text{mean dose in PTV} \quad (4)$$

Many authors have reported investigations on Lung SBRT treatment plan quality by analyzing adherence to the various goals set forth in the RTOG protocols.^{12–16} Treatment planning outcomes

have complex dependencies on many factors, both PTV and OAR related. However, we believe there are two important PTV-related planning considerations that may have been underappreciated in this large body of work. Our analyses have indicated that both the PTV mean dose (PTV D_{av}) and the PTV surface area (SA_{PTV}) can offer important guidance in the treatment planning process. Therefore, the goal of this study is to develop an understanding of the behavior of R50% on these two PTV characteristics in a carefully controlled, systematic process that excludes complications resulting from a consideration of the full array of planning objectives. As such, any guidance derived from this study is intended to augment the planning process and not serve as a radical alteration. To achieve the study goals, we have utilized an anthropomorphic phantom model that allows a controlled environment to independently evaluate the effects PTV D_{av} and SA_{PTV} have on the plan metric R50%. We also derive a clinically useful and physically reasonable R50% lower bound that illuminates the dependence of R50% on SA_{PTV}.

2 | MATERIALS AND METHODS

This study utilized a treatment planning CT of the IROC Thorax-Lung Phantom[®] (IROC Houston QA Center, Houston, TX) as the anthropomorphic phantom model. Complications from patient motion were not considered. We ignore the IROC PTV in the left lung and create a unique set of PTVs in the right lung with well-controlled characteristics, eg, specific contour shape, dimensions, and overriding the electron density within the contour to create a uniform density of 0.9 g/cc. All treatment planning was performed on an Eclipse Radiation Treatment Planning System (RTPS) (Varian Medical Systems, Palo Alto, CA) using photon optimizer v15.6 with a final calculation via the AAA v15.6 algorithm on a 1 mm calculation grid size. Plans were created for delivery on a Varian TrueBeam STx[®] with 120 leaf HD MLC. None of the plans utilized in the study were subjected to standard QA procedures, but the RTPS and its model of the delivery system have been clinically validated by the IROC using the onsite planning and treatment delivery protocol for the Thorax-Lung Phantom[®] and many direct patient QA measurements of clinical Intensity Modulated Radiation Therapy (IMRT), SBRT, and cranial SRS patient cases. All plans use Volumetric Modulated Arc Therapy (VMAT, RapidArc[®]) techniques. The arc geometry was limited to include only the PTV and right lung and used typical clinical arc limits and collimator angles.

All PTVs were created as simple geometric shapes of uniform physical density to simplify the problem and control as many variables as possible, thus isolating the PTV characteristics under study. The simple, well-defined geometric shapes also allowed an analytic calculation of the PTV surface area.

The geometric configuration of gantry, collimator, and phantom is shown in Fig. 1. All plans in this study are RapidArc 2-arc VMAT plans having gantry angle limits between 30° and 181° and collimator angles of 45° or 330°.

All plans use a typical SBRT prescription (Rx) of 50 Gy in five fractions, and it was required that 95% of the PTV volume receive

the Rx dose (ie, D95% condition).^{17,18} The AAA algorithm was used in part because it is the most common clinical calculation algorithm in Eclipse. There is justification for this choice in an evaluation performed by Matsuoka et al.¹⁹ showing good precision for determination of the quantity $V_{50\%}/V_{100\%}$, a quantity similar to R50%. In addition, Matsuoka et al. showed that for SBRT targets with near uniform density, various dose indices such as $D_{95\%}$ and $D_{50\%}$ are essentially independent of dose calculation algorithm. Therefore, our phantom study with no respiratory motion and well-defined target properties satisfies these conditions. All plans meet the requirements of RTOG protocols⁷⁻⁹ for D2cm, V105%, and CI.

2.A | R50% dependence on PTV Dose Heterogeneity

To study the relationship between R50% and PTV dose heterogeneity, we generated four spherical volumes (9, 33, 53, and 81 cc) and four cylindrical shapes of the same volumes but varying elongation. We employed two different PTV shapes to control for PTV shape so the results for dose heterogeneity study can be clearly attributed to the dose heterogeneity independent of the PTV shape. All eight PTVs are located in the center of the right lung. The density of the PTVs was overridden to a typical 0.9 g/cc for all cases.

A series of ten plans for each PTV were created that control the PTV dose heterogeneity using only a PTV maximum dose constraint (PTV D_{max}) and the prescription D95% condition. The PTV D_{max} constraint included an unlimited maximum dose and maximums ranging from 140% to 100% of the Rx dose decreasing in increments of 5%. This resulted in plans with progressively more dose homogeneity in

the PTV. We use PTV D_{max} to contain the PTV dose heterogeneity within the limits of the prescription D95% and PTV D_{max} . We examine these results in light of two more standard metrics for dose heterogeneity: ICRU HI and RTOG HI [defined by Eqs. (2) and (3), respectively]. We also study these results with a third metric PTV D_{av} defined by Eq. (4).

We report the results relative to PTV D_{av} because this is a reasonable measure of the actual global dose delivered to the target. D_{av} is also a readily available parameter in all commercially available RTPS and allows comparison with previous studies.

To further understand the dose distribution, we examined the average dose in the shell of the IDC50% that is outside the PTV. For notational simplicity, we define IDC50%shell as that part of IDC50% that is not part of the PTV.

$$IDC50\%_{shell} = IDC50\% - PTV \quad (5)$$

This evaluation of PTV dose heterogeneity generated a total of 80 plans (4 volumes \times 2 shapes \times 10 D_{max} constraints).

2.B | Dependence on PTV surface area

To study the relationship between R50% and SA_{PTV} , we generated a large set of PTVs of both spherical and cylindrical shape and having varying surface area. All PTVs were defined to have a uniform density of 0.9 g/cc. The optimizer PTV D_{max} constraint was held constant at 120% of prescription yielding a PTV D_{av} of approximately 110% of Rx.

With reference to RTOG 0915,⁹ we generated 11 spherical PTVs ranging in volume from 2 to 163 cc denoted as "Sphere" (or "Sph").

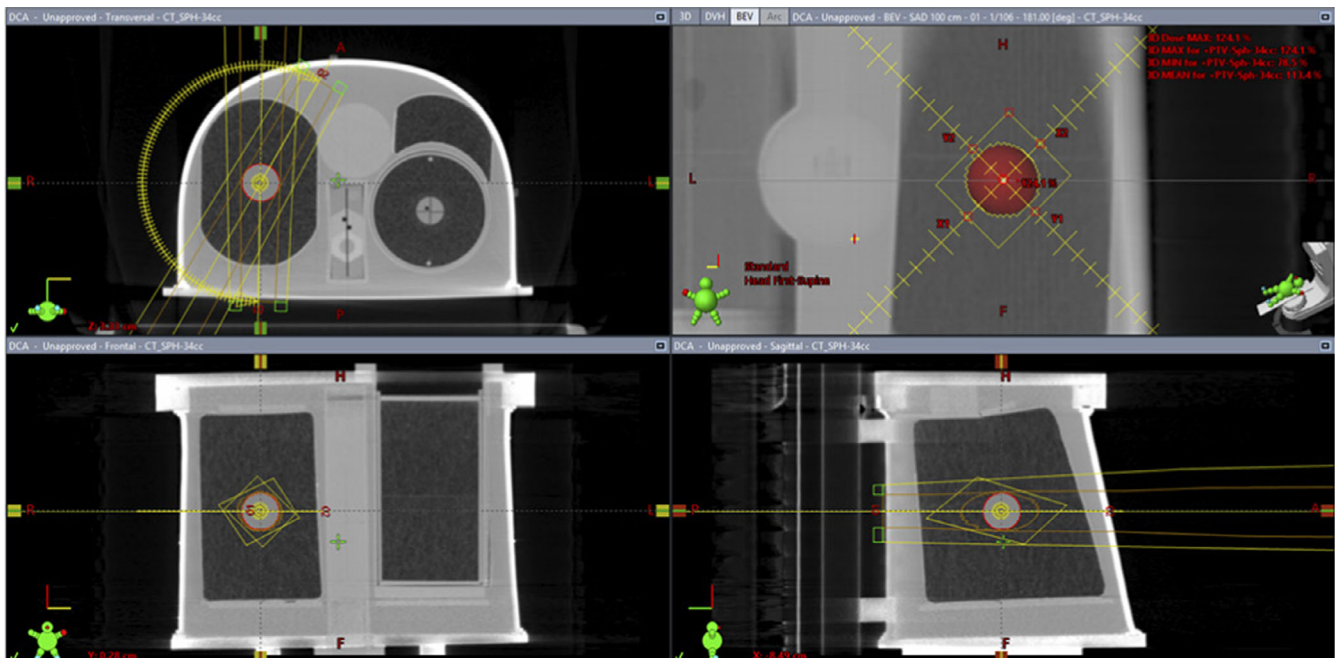


FIG. 1. Geometry of the experimental plans run on the IROC Thorax-Lung Phantom[®]. The PTV shown in the right lung is a density override volume and indicates the position of isocenter and the arc geometry used.

A set of cylindrical PTVs were generated having volumes equal to the 11 spherical PTVs and a maximum length equivalent to the maximum dimension given in RTOG 0236 thus fixing diameter for a given maximum length. These cylinders were placed in 2 distinct orientations: cylindrical axis in the superior/inferior direction (denoted as "RTOG Horizontal Cylinders" or "RTOG Horz Cyl"); and a second set with the cylindrical axis in the anterior/posterior direction (denoted as "RTOG Vertical Cylinders" or "RTOG Vert Cyl"). To provide additional variation in the surface area, we created an additional set of cylindrical PTVs with the same volume as the spherical PTVs but very long cylindrical axes and thus smaller radial dimensions than the cylindrical PTVs mentioned above. The maximum cylinder height was capped at 8 cm, however, to avoid clinical irrelevance. These new cylinders are also oriented in both the "horizontal" and "vertical" directions previously described. The dual cylinder orientations were used to more directly test the PTV surface area dependence of R50%, by controlling for PTV orientation relative to the delivery geometry of the beams. This section of the study generated a total of 55 PTVs and associated plans.

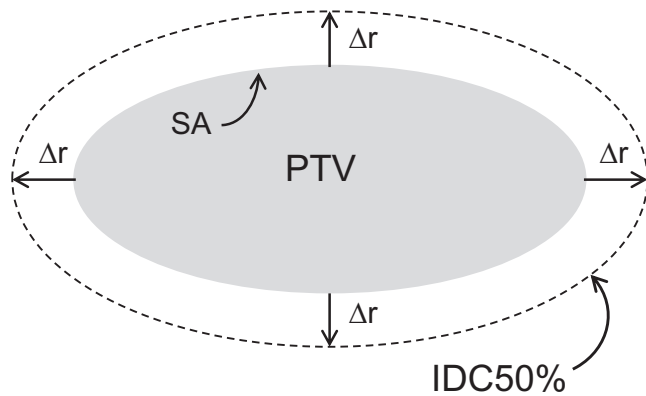
2.C | R50% Limit Derivation

To derive the R50% limit in highly conformal treatment like SBRT, begin by considering Fig. 2.

The volume of the IDC50% can be determined by a differential shell expansion of the PTV. If the expansion is vanishingly small, Δr becomes dr . In this differential shell, the volume is given by

$$\text{Volume of Differential Shell}_1 = V_1 = SA_{PTV} \times dr \quad (6)$$

This is strictly correct only if the differential shell is truly an infinitesimal expansion. This expansion generates a new volume and that volume, V_1 , has a surface area, SA_1 . Now that volume, V_1 , can be expanded by another dr into volume V_2 .



Δr = distance of uniform expansion of the PTV that achieves the IDC50%

Fig. 2. An arbitrary shape planning target volume of surface area SA is expanded by Δr to achieve the IDC50% volume.

$$V_2 = SA_1 \times dr \quad (7)$$

V_2 has a surface area SA_2 , and

$$SA_2 > SA_1 \quad (8)$$

This process continues through the entire infinitesimal differential shell series of nested shells such that

$$SA_{(i+1)} > SA_i \quad (9)$$

Thus, SA is a function of r , $SA(r)$, where we are concerned with r in the range from the PTV surface outward. For notational simplicity, adopt the notation that $r = 0$ at the surface of the PTV, and $r = \Delta r$ at the surface of IDC50%.

Continue adding differential shells until the surface reaches IDC50% (at distance Δr). Thus, strictly speaking,

$$V_{IDC50\%} = V_{PTV} + \int_0^{\Delta r} SA(r) dr \quad (10)$$

Since each differential shell surface area is larger than the one nested inside it, one can see that

$$V_{IDC50\%} > V_{PTV} + SA_{PTV} \times \Delta r \quad (11)$$

Divide both sides of the inequality by V_{PTV} to obtain the following:

$$R50\% > 1 + \frac{SA_{PTV}}{V_{PTV}} \times \Delta r \quad (12)$$

We can now define a lower bound for R50%. This lower limit we name $R50\%_{min_{\Delta r}}$.

$$R50\%_{min_{\Delta r}} = 1 + \frac{SA_{PTV}}{V_{PTV}} \times \Delta r_{min} \quad (13)$$

Values of Δr_{min} are difficult to determine analytically, but estimates can be obtained from previous lung SBRT treatment planning studies. For example, Hoffman et al.²⁰ determined lung SBRT Gradient Measure (GM) values obtained from a multicenter analysis of 317 lung SBRT plans. They define GM as the difference, in centimeters, of the equivalent sphere radii of the 50% and 100% isodose volumes ($R_{eq}^{50\%}$ and $R_{eq}^{100\%}$, respectively). Thus,

$$GM = R_{eq}^{50\%} - R_{eq}^{100\%} \quad (14)$$

By comparison, for a perfectly conformal plan with Conformality Index = 1, the volume of the 100% isodose volume is identical to and spatially coincident with the PTV volume. Thus, for the equivalent sphere, $R_{eq}^{100\%}$ = radius of the equivalent sphere PTV. In such case, the GM is equivalent to the Δr as defined in Fig. 2. Thus, the GM values from Hoffman et al can be used as approximations to our Δr_{min} . The GM values obtained from Hoffman, et al. are binned by PTV Volume and range from 0.84 to 2.13 cm for 1.8–3.8 cc to >163 cc, respectively. So, Eq. (13) becomes:

$$R50\%_{\min_{GM}} = 1 + \frac{SA_{PTV}}{V_{PTV}} \times GM \quad (15)$$

where the subscript GM designates $\Delta r_{\min} = GM$ from Hoffman et al. (Ref. [20], Table 1]).

In principle, the limit in Eq. (13) should hold true even if the value of Δr is refined for different clinical presentation and different densities in the IDC50%shell, such as SBRT for liver, spine, or even cranial SRS.

3 | RESULTS

3.A | R50% dependence on PTV D_{av}

The PTV dose heterogeneity can be described in many ways. Figure 3 shows three different descriptions of PTV dose heterogeneity: ICRU HI, RTOG HI, and PTV D_{av} expressed as a percentage of the prescription dose. The PTV shape (sphere or cylinder) has very little effect on the overall trend, thus, the trend is attributable to the dose heterogeneity alone. It is clear from these plots that each measure of heterogeneity contains very similar information. PTV D_{av} is reported directly by all commercially available RTPS and is easy to conceptualize. In addition, D_{av} is directly correlated with tumor control.¹⁷ Therefore, we choose PTV D_{av} as our metric of choice for the evaluation of PTV dose heterogeneity. Results for the dependence of R50% on PTV D_{av} are summarized in Fig. 4.

The three regions of interest seen in all four panels of Fig. 4 are PTV $D_{av} < 105\%$ Rx, PTV $D_{av} > 115\%$ Rx, and the interval between 105% and 115% Rx. There appears to be a relatively broad local minimum in R50% in the interval between 105% and 115% with increases outside this range. The R50% local minimum region as a function of PTV D_{av} (between 105% and 115% of the Rx dose) appears to vary slightly with PTV volume. The R50% local minimum as a function of PTV D_{av} occurs at $D_{av} \approx 110\%$ Rx.

We also examined the mean dose in the IDC50%shell. Figure 5 shows that as PTV D_{av} decreases below the local minimum ($D_{av} \approx 110\%$), the mean dose in the IDC50%shell increases for all PTV volumes, ie, the dose spill outside the PTV increases as the PTV dose becomes more homogeneous.

3.B | Dependence on PTV surface area

The results of the PTV surface area study are summarized in Figs. 6 and 7. Figure 6 shows R50% for all 55 plans plotted as a function of the SA_{PTV}/V_{PTV} for all volumes and PTV shapes (spheres and various cylinders). Also displayed is the numerical value of $R50\%_{\min_{GM}}$ [Eq. (15)], which is the limit $R50\%_{\min_{\Delta r}}$ that uses $\Delta r_{\min} = GM$ values given by Hoffman, et al.²⁰ Notice that the lower bound $R50\%_{\min_{GM}}$ is always less than the planned R50% and thus is indeed a lower bound.

Figure 7 provides the same data as Fig. 6 but alternatively plotted as a function of PTV volume. As seen in Fig. 7(a), R50% rises sharply as the PTV Volume approaches zero. Again, it is evident that

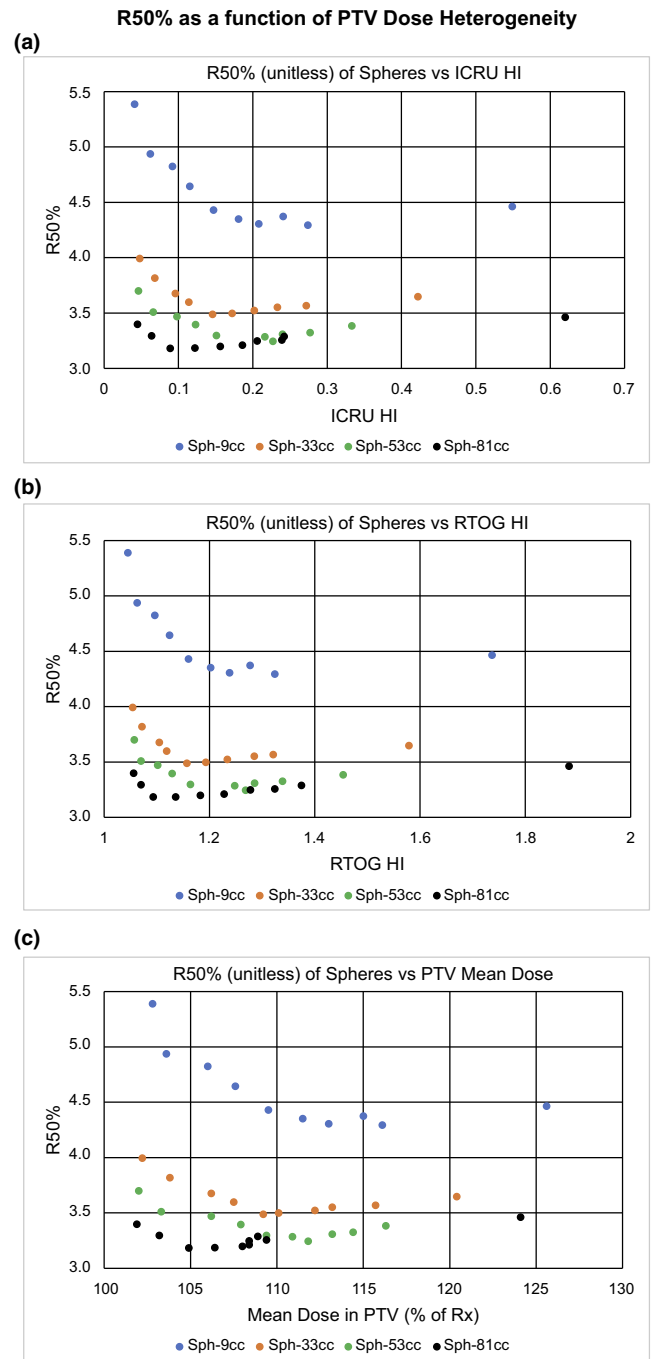


FIG. 3. R50% as a function of planning target volume (PTV) dose heterogeneity. Plots of R50% as a function of various measures of PTV dose heterogeneity. (a) R50% vs ICRU HI. (b) R50% vs RTOG HI. (c) R50% vs PTV Mean Dose (PTV D_{av}) expressed as a percentage of the prescription dose.

the $R50\%_{\min_{GM}}$ appears to be a true lower bound for R50% regardless of PTV volume. Figure 7(b) is a magnified view of a limited range of the data in 7(a). Here, one can see a vertical stacking of the R50% values that depends on the SA_{PTV} for the same nominal V_{PTV} . R50% and SA_{PTV} for various PTV shapes and orientations are summarized in Table 1 for a nominal $V_{PTV} = 34$ cc. The dependence of R50% on SA_{PTV} is evident and consistent with the trend seen for

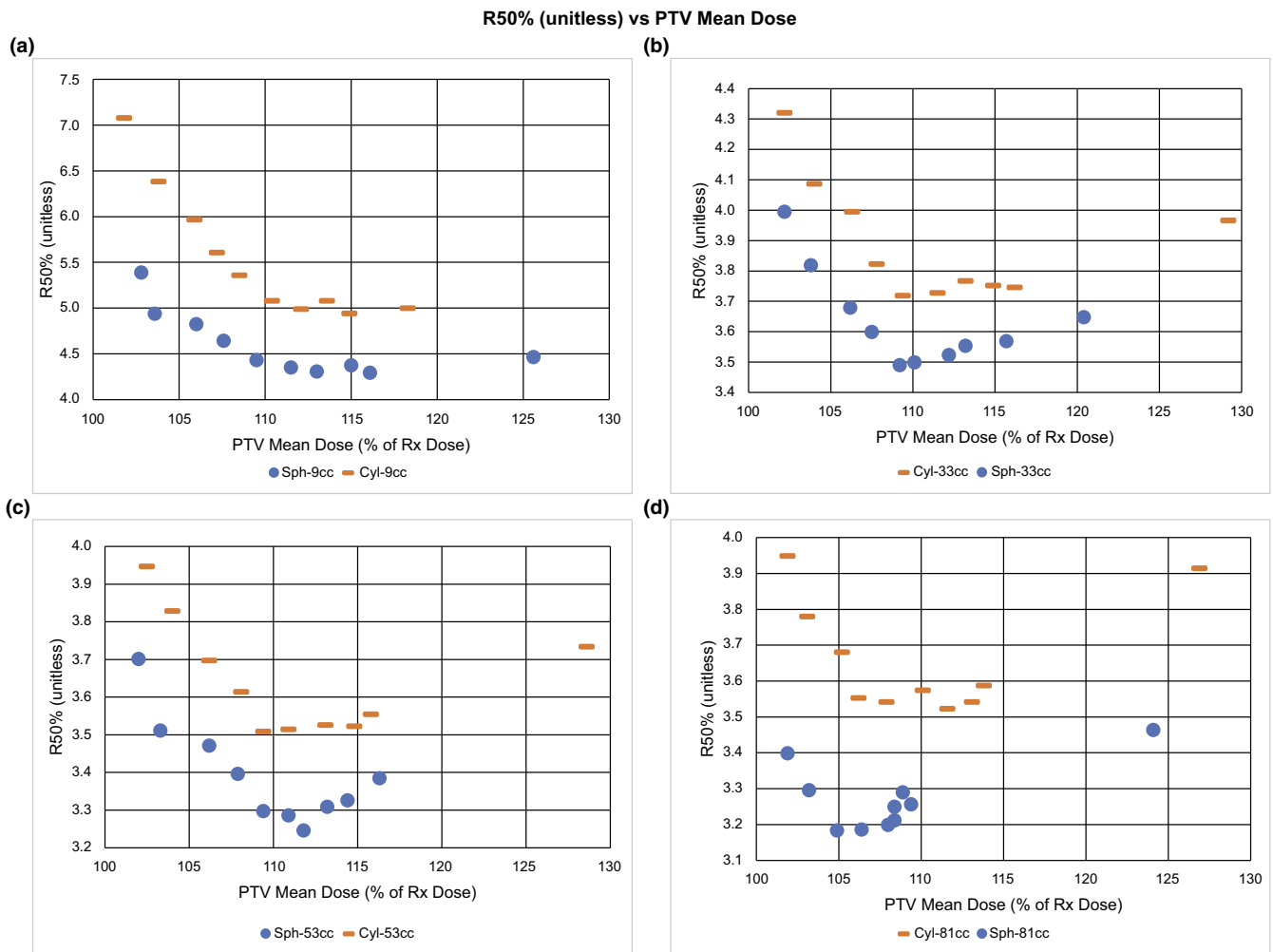


FIG. 4. R50% (unitless) vs planning target volume (PTV) mean dose. Plots of R50%(unitless) vs PTV Mean Dose (D_{av}) as % of Rx Dose for a tissue equivalent PTV density (0.9 g/cc) of both spherical and cylindrical shapes for volumes: (a) 9 cc, (b) 33 cc, (c) 53 cc, and (d) 81 cc. Note the minimum in R50% that occurs near $D_{av} = 110\%$ of Rx dose for all volumes and shapes.

the 34 cc volume in Fig. 7(b). That is, the largest SA_{PTV} corresponds to the largest R50% value. For a given cylindrical SA_{PTV} value, the orientation of the cylinder axis does play some role in the plan R50% obtained. It should be noted that the actual volume of the PTVs may not be exactly 34 cc due to voxel discretization limitations in the RTPS.

4 | DISCUSSION

4.A | R50% dependence on PTV D_{av}

The observed R50% local minimum in PTV D_{av} seen in Fig. 4 can also be seen in the results of previous work.^{12,21} However, these and other studies made little comment about the phenomenon. This R50% local minimum in PTV D_{av} is an interesting result of this study. The R50% local minimum region as a function of PTV D_{av} occurs between 105% and 115% of the Rx dose and appears to vary slightly with PTV volume. We are not certain that this minimum behavior will hold when other treatment planning constraints are

applied, but it is a possible characteristic in a general treatment planning scenario.

The R50% local minimum as a function of PTV D_{av} as shown in Fig. 4, implies that there are two processes at work. One process dominates at the high end where PTV D_{av} is large while a different process dominates when PTV D_{av} is low. Where PTV D_{av} is large, the general result that R50% is increased seems reasonable given that more photon energy fluence is required to deliver a higher PTV mean dose. This higher photon energy fluence results in larger entrance doses around the PTV likely contributing to the larger R50%. On the low PTV D_{av} end, the rise in R50% as the PTV dose homogeneity increases may be explained by the photon energy fluence distribution. Because these are VMAT RapidArc plans, to achieve a more homogeneous PTV dose while maintaining the D95% prescription, the optimizer must force dose out of the PTV center and into the PTV periphery. This allows for the dose to the PTV center to remain close to the prescription dose while increasing the dose in the periphery to a level consistent with prescription dose. The PTV is effectively very thin at the periphery and so there

Mean Dose of IDC50%shell vs PTV Mean Dose

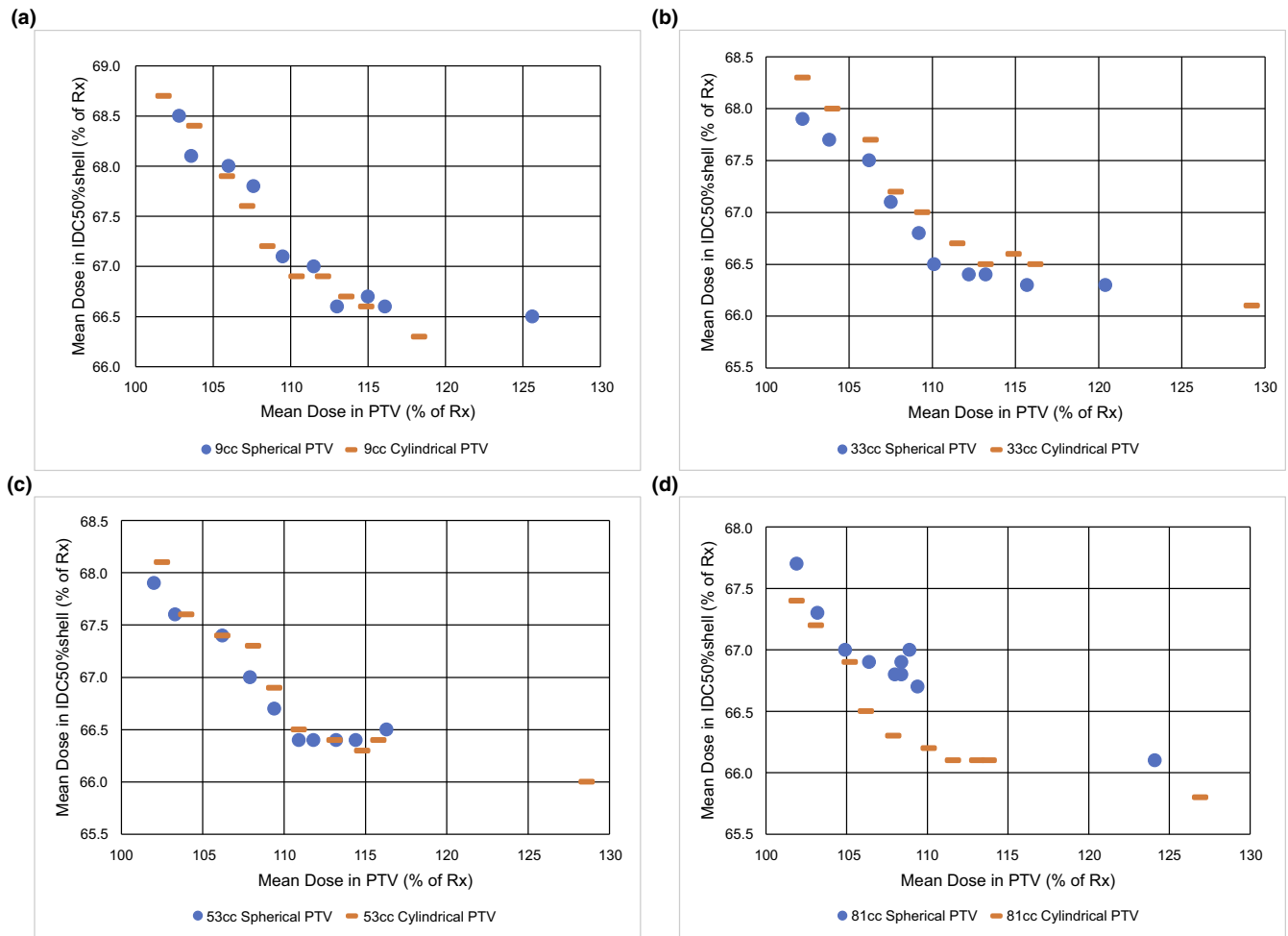


FIG. 5. Mean dose of IDC50%shell vs planning target volume (PTV) mean dose. Plots of IDC50%shell Mean Dose vs PTV Mean Dose (D_{av}) as percent of prescription Dose (% of Rx) for a tissue equivalent PTV (0.9 g/cc) of both spherical and cylindrical shapes for volumes: (a) 9 cc, (b) 33 cc, (c) 53 cc, and (d) 81 cc. Note the marked increase in IDC50%shell Mean Dose as the PTV D_{av} approaches the Rx dose.

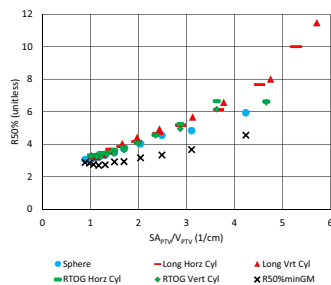


FIG. 6. The graph $R50\%$ vs SA_{PTV}/V_{PTV} showing all 55 plans of the Surface Area study. Also shown is $R50\%_{minGM}$ [Eq. (15)] using the GM values from Hoffman et al.²⁰ Notice that the lower bound $R50\%_{minGM}$ is always $<R50\%$ for all plans and thus is indeed a lower bound.

is less PTV material to absorb the beam. This would increase the exit fluence from the PTV periphery. The higher exit fluence would contribute to a larger $R50\%$ and, thus, more dose would be deposited in the IDC50%shell. This effect is illustrated in Fig. 5 where the dose in

the IDC50%shell is seen to increase as the dose in the PTV becomes more homogeneous as indicated by a reduction in the PTV D_{av} . We acknowledge that there is little clinical justification for seeking a homogeneous PTV dose in SBRT. One could even argue that this is contrary to the standard clinical practice of SBRT. Previous recommendations⁵ have encouraged doses as high as 130% of Rx in the PTV. The point of this study, however, is to understand the effect that PTV dose heterogeneity, quantified by PTV D_{av} , has on $R50\%$. Many previous studies have shown how a heterogeneous dose within the PTV is desirable for a steep dose falloff surrounding PTV.^{13–16,22,23} Our study clearly shows that this forced dose heterogeneity may only be useful to a point, that being the $R50\%$ local minimum in PTV D_{av} . Beyond this point, increasing the PTV dose heterogeneity will increase the $R50\%$. Many of the steep dose falloff studies are for cranial radiosurgery targets.^{14–16,22,23} Most of the radiosurgery target volumes are <10 cc and many involve SRS cones or a GammaKnife delivery platform. It is conceivable that the exact location of the $R50\%$ local minimum in PTV D_{av} could be optimizer and delivery technique dependent.

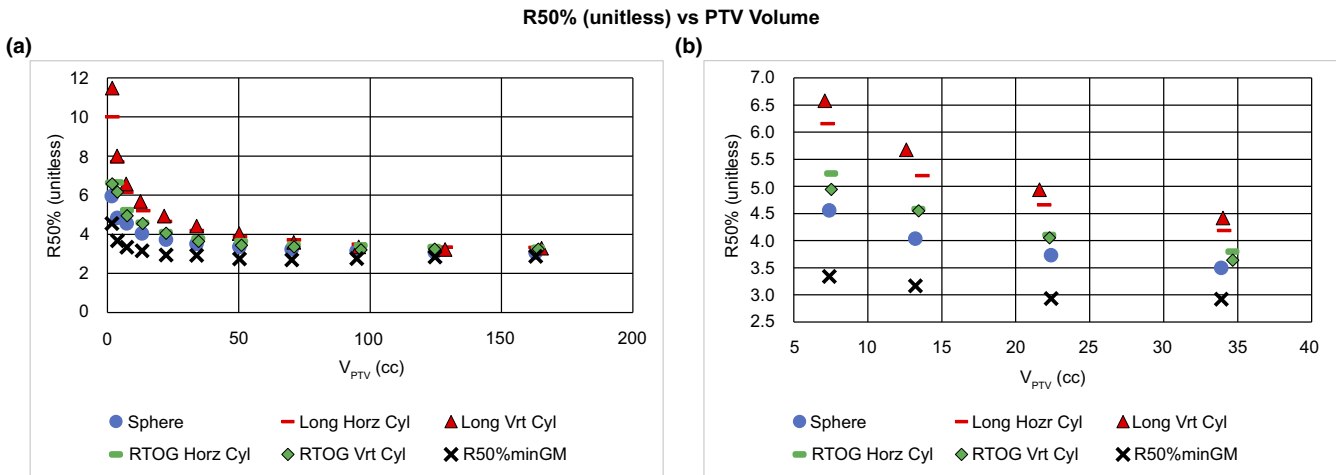


FIG. 7. R50% (unitless) vs planning target volume (PTV) volume. The standard graph of R50% vs V_{PTV} for all 55 plans of the Surface Area study. Also graphed is $R50\%_{minGM}$ [Eq. (15)] obtained using the GM values from Hoffman et al.²⁰ (a) The full dataset. Notice that the lower bound $R50\%_{minGM}$ is always less than R50% for all plans and thus is indeed a lower bound. (b) Is a highly magnified version of the same plot to demonstrate the vertical stacking of the R50% values for nearly the same volume. This vertical stacking corresponds to the Surface Area (SA) of the individual PTVs with some cylinder orientation evident as a perturbation on the larger surface area effect.

TABLE 1 Results from Surface Area study for planning target volumes (PTVs) having a nominal volume of 34 cc. Notice the association with the stack of points at about 34 cc as shown in Fig. 6(b). There is also a second-order effect of cylinder orientation on R50%. Note that a larger SA_{PTV} correlates with a larger R50% for the same volume.

PTV description	SA_{PTV}	R50%	Actual V_{PTV}
Long Vrt Cyl	67.0	4.42	34.1
Long Horz Cyl	67.0	4.18	34.1
RTOG Horz Cyl	59.0	3.79	34.7
RTOG Vrt Cyl	59.0	3.64	34.7
Sphere	50.8	3.50	33.9

It should be noted that the difference between the spherical and cylindrical PTVs in Fig. 4 shows roughly the same local minimum in R50%. This implies that the local minimum observed is consistent regardless of PTV shape. The differences between the spherical and cylindrical PTVs are exposed in the study of PTV surface area.

The immediate clinical effect of this study is to alert the treatment planner that both homogenous PTV doses and extreme heterogeneous PTV dose distributions are undesirable if the goal is to obtain optimal values of R50%. Dosimetrists, Physicists, and Physicians need to be aware of this phenomenon.

4.B | Dependence on PTV surface area

Dependence of R50% on SA_{PTV} appears to be underreported in the literature. The results of the PTV surface area study are illustrated in Fig. 6. R50% is seen to be highly correlated with SA_{PTV}/V_{PTV} and very nearly linear regardless of PTV shape. One would expect this result from the $R50\%_{min\Delta r}$ expression given by $R50\%_{min\Delta r} = 1 + \frac{SA_{PTV}}{V_{PTV}} \times \Delta r_{min}$ [Eq. (13)]. This clearly establishes the

relationship of R50% to both volume of the PTV and the surface area of the PTV. However, there is also a slight curvature to the distribution owing to the PTV Volume dependence of $\Delta r = GM$ that was observed in the clinical data of Hoffman et al.²⁰ This Δr dependence on PTV Volume is also visible in the $R50\%_{minGM}$ lower bound.

The spherical PTVs always have the smallest R50% of any given volume. A sphere also has the smallest surface area to volume ratio of any three-dimensional geometric object of arbitrary shape. Again, this supports the correlation of SA_{PTV} to R50% that one would expect from Eq. (13).

The data in Fig. 6 are clustered for small values of SA_{PTV}/V_{PTV} in part because, for the larger volume geometric figures, the surface area to volume ratio naturally decreases and shape becomes less important. Furthermore, because of limitations placed on the PTVs when they were created, the cylinders all converge toward having a diameter \approx height, which is the minimum surface area configuration of a cylinder. The larger values of SA_{PTV}/V_{PTV} correlate with the smaller volume PTVs. For small 3D volumes, the SA_{PTV}/V_{PTV} ratio becomes higher and diverges more for spheres and cylinders. These aspects of the data are also predicted by Eq. (13).

The gradient metric (GM) differs slightly from the Δr of $R50\%_{min\Delta r}$ in that GM is calculated using effective spheres, not the actual shape of the PTV. Thus, GM will correlate better with Δr for a spherical PTV than for a cylindrical PTV. The actual Δr is likely dependent on the delivery geometry, so different treatment machines probably have slightly different Δr values. This hypothesis would predict that a highly noncoplanar delivery from a CyberKnife (Accuray, Sunnyvale, CA) would have a smaller Δr because the treatment delivery geometry could be optimized to the specific PTV shape.

One can investigate the limits of $R50\%_{min\Delta r}$ by examining the extremes of $\Delta r = r_{50} - r_{100\%}$. If $\Delta r = 0$ (indicating an infinitely steep,

physically impossible dose drop-off), one sees that in Eq. (13), $R50\%_{\min_{\Delta r}} = 1$ indicating that the $IDC50\% = IDC100\%$. Clearly this is the absolute unphysical limit of R50% when $IDC50\% = PTV$ Volume. Furthermore, one sees that if Δr is very large, the $R50\%_{\min_{\Delta r}}$ would be governed more strongly by SA_{PTV}/V_{PTV} . This is more likely to be true for lung SBRT, where the $IDC50\%_{\text{shell}}$ is low-density lung with a low electron stopping power, than for cranial SRS or liver SBRT where the $IDC50\%_{\text{shell}}$ is soft tissue, and thus higher electron stopping power.

It is also likely that Δr is dependent on the average aperture size as determined by the optimizer. For larger PTVs, the average aperture size would typically be larger and thus we would predict that Δr is larger for large PTVs. The converse would be expected true for small PTVs. Of course, this is the result as reported by Hoffman et al.²⁰ through their GM values.

The relationship $R50\% > 1 + SA_{PTV}/V_{PTV} \times \Delta r$ also suggests that when assessing two PTVs of the same volume, the PTV with the larger surface area will have larger R50%. This accounts, in part, for the vertical spread of the R50% data in Fig. 7 that appear as a vertical stack of different plan data points of same/similar volume and is demonstrated in Table 1 for one case ($V_{PTV} \approx 34$ cc).

We also note similarity of the PTV surface area study results to the recent publication of Goldbaum et al.²⁵ working in cranial SRS. In that work, the authors hypothesized that "an increase in TV12 [intermediate dose spill] could be related to an increase in the surface area of the target, and the surface area of the target could be quantified by analogy with an ellipsoid."²⁵ Their attempt to use effective ellipsoids to quantify the PTV surface area did not prove productive. However, as we see from this work, the PTV surface area is a decisive factor in predicting the R50% limit given by $R50\%_{\min_{\Delta r}}$.

The results shown in Fig. 7(a) are markedly similar to clinical results published previously: Ref [26, Fig. 3], Ref [20, Fig. 3], Ref [24, Fig. 4], and Ref [11, Fig. 1(b)]. These other publications make no specific comment about the origin of this overall trend. This work, however, provides a clinically useful and physically reasonable explanation of the trend in R50% as a function of V_{PTV} . The smaller surface area PTV (sphere) always has a smaller R50% for any given PTV volume. Furthermore, this general PTV surface area trend is maintained even when cylinders are oriented differently as shown in Table 1. Thus, the PTV orientation is only a minor perturbation on the overall PTV surface area effect.

Considering what the PTV surface area represents, it should not be surprising that PTV surface area has a marked effect on R50% because the PTV surface area is a direct measure of how much non-target tissue is exposed to the high dose of the PTV: PTV surface area is the interface between target and nontarget tissue. Given the same degree of conformality, a larger PTV surface area in a lung SBRT plan means more lung tissue is exposed to the highest dose region. That exposure would propagate out to all isodose lines outside the target including the 50% isodose line defining the R50%.

Since PTV surface area markedly affects R50%, it would be advantageous to know this value in all clinical situations. At present we are aware of no commercially available RTPS that can report the

surface area of a segmented structure. This may be why the importance of surface area has not been previously recognized. Having this statistic available in the treatment planning systems would make the study of PTV surface area possible in clinical studies.

Other authors have observed PTV shape dependence²⁷ and have noted that a concave PTV has a higher R50% than a comparable volume fully convex PTV. Naturally, a concave PTV will have a higher surface area than a convex PTV of same volume. PTV surface area may prove a useful metric in future studies involving PTV shape.

The immediate clinical impact of this PTV surface area study is the understanding that for PTV shapes that are distinctly non-spheroidal, the R50% will be larger for the same volume and thus it will be more difficult to meet the R50% criterion given in the RTOG protocols⁷⁻⁹ for such plans. The derived $R50\%_{\min_{GM}}$ [Eq. (15)] is clinically useful in its own right. But it also clearly establishes the relationship of R50% with the PTV surface area (SA_{PTV}).

The two PTV characteristics, PTV D_{av} and SA_{PTV} , have a marked impact on the value of R50% and can be summarized as follows:

PTV Mean Dose (D_{av}): Heterogeneity in the PTV dose distribution, as indicated by PTV D_{av} , affects the value of R50%. There is a local minimum in R50% for PTV $D_{av} \approx 110\%$ prescription dose.

PTV Surface Area: As the PTV surface area increases, the R50% naturally increases if the PTV volume stays the same.

The principle goal of this work is to illuminate the effects of the PTV characteristics, PTV D_{av} , and SA_{PTV} , on the plan metric R50% and to develop a conceptual understanding of these effects. This will allow future investigations to be more detailed and discuss how the entanglement of other characteristics is affecting the in-depth study of a single PTV characteristic.

5 | CONCLUSIONS

This research has identified two critical characteristics of the PTV that have not been clearly articulated in the vast body of previous research in lung SBRT: PTV D_{av} and SA_{PTV} . Equation (13) clearly establishes a relationship between R50% and SA_{PTV} that has not been fully appreciated previously. This research provides new insight on a large body of previously published work related to lung SBRT. A better understanding of the relationship of these PTV characteristics to the ultimate R50% could provide improved guidance for determining when an optimal SBRT plan is achieved. Future work will provide more detailed descriptions of how these PTV characteristics affect R50%.

ACKNOWLEDGMENTS

The authors would like to thank Debra Olson Desai, MS for her assistance with the editing and organization of the References, her work formatting the graphs, and formatting the equations. Ulrich Langner, PhD is acknowledged for his critical review of a very early version of the manuscript. Dharmin Desai would like to thank his mentors, Dr. Lee Johnson and Dr. Robert Zwicker. They have

selflessly shared their knowledge with him through in-depth discussions and insightful advice.

CONFLICT OF INTEREST

None of the authors of this research have conflicts of interest to disclose.

REFERENCES

- Guckenberger M, Andratschke N, Alheit H, et al. Definition of stereotactic body radiotherapy: principles and practice for the treatment of stage I non-small cell lung cancer. *Strahlenther Onkol*. 2014;190:26–33.
- Soldà F, Lodge M, Ashley S, et al. Stereotactic radiotherapy (SABR) for the treatment of primary non-small cell lung cancer: systematic review and comparison with a surgical cohort. *Radiother Oncol*. 2013;109:1–7.
- Hörner-Rieber J, Bernhardt D, Blanck O, et al. Long-term follow-up and patterns of recurrence of patients with oligometastatic NSCLC treated with pulmonary SBRT. *Clin Lung Cancer*. 2019;20:e667–e677.
- Talapatra K, Majumder D, Chadha P, et al. Stereotactic body radiotherapy for lung tumors: dosimetric analysis and clinical outcome. *Indian J Cancer*. 2018;55:170–175.
- Timmerman R, Paulus R, Galvin J, et al. Stereotactic body radiation therapy for inoperable early stage lung cancer. *JAMA*. 2010;303:1070–1076.
- Timmerman R, Herman J, Cho L. Emergence of stereotactic body radiation therapy and its impact on current and future clinical practice. *J Clin Oncol*. 2014;32:2847–2854.
- Timmerman R. Stereotactic Body Radiation Therapy for Inoperable Early Stage Lung Cancer. *JAMA*. 2010;303:1070. <http://dx.doi.org/10.1001/jama.2010.261>
- Bezjak A, Paulus R, Gaspar L. E., et al. Safety and Efficacy of a Five-Fraction Stereotactic Body Radiotherapy Schedule for Centrally Located Non-Small-Cell Lung Cancer: NRG Oncology/RTOG 0813 Trial. *Journal of Clinical Oncology*. 2019;37 (15):1316–1325. <http://dx.doi.org/10.1200/jco.18.00622>
- Videtic G, Hu C, Singh AK, et al. A randomized phase II study comparing 2 stereotactic body radiation therapy (SBRT) schedules for medically inoperable patients with stage I peripheral non-small cell lung cancer. *NRG Oncology*. 2010;93:757–764.
- Yang J, Fowler J, Lamond J, et al. Red shell: defining a high-risk zone of normal tissue damage in stereotactic body radiation therapy. *Int J Radiat Oncol Biol Phys*. 2010;77:903–909.
- Yarpalvi R, Garg MK, Shen J, et al. Evaluating which plan quality metrics are appropriate for use in lung SBRT. *Br J Radiol*. 2018;91:20170393.
- Bell J, Patel P, Higgins K, et al. Fine-tuning the normal tissue objective in eclipse for lung stereotactic body radiation therapy. *Med Dosim*. 2018;43:344–350.
- Hong L, Garg M, Lasala P, et al. Experience of micromultileaf collimator linear accelerator based single fraction stereotactic radiosurgery: tumor dose inhomogeneity, conformity, and dose fall off. *Med Phys*. 2011;38:1239–1247.
- Ohtakara K, Hayashi S, Tanaka H, Hoshi H. Consideration of optimal isodose surface selection for target coverage in micro-multileaf collimator-based stereotactic radiotherapy for large cystic brain metastases: comparison of 90%, 80% and 70% isodose surface-based planning. *Br J Radiol*. 2012;85:e640–e646.
- Zhao B, Jin J, Wen N, et al. Prescription of 50–75% isodose line may be optimum for linear accelerator based radiosurgery of cranial lesions. *J Radiosurg SBRT*. 2014;3:139–147.
- Clark G, Popple R, Young P, Fiveash J. Feasibility of single-isocenter volumetric modulated arc radiosurgery for treatment of multiple brain metastases. *Int J Radiat Oncol Biol Phys*. 2010;76:296–302.
- ICRU Report 91: prescribing, recording, and reporting of stereotactic treatments with small photon beam. *J ICRU*. 2014;14:1–160.
- Benedict S, Yenice KM, Followill D, et al. Stereotactic body radiation therapy: the report of AAPM Task Group 101. *Med Phys*. 2010;37:4078–4101.
- Matsuoka T, Araki F, Ohno T, et al. Dependence of volume dose indices on dose calculation algorithms for VMAT-SBRT plans for peripheral lung tumor. *Med Dosim*. 2019;44:284–290.
- Hoffman D, Dragojević I, Hoisak J, et al. Lung stereotactic body radiation therapy (SBRT) dose gradient and PTV volume: a retrospective multi-center analysis. *Radiat Oncol*. 2019;14:162.
- Chan M, Wong M, Leung R, et al. Optimizing the prescription isodose level in stereotactic volumetric-modulated arc radiotherapy of lung lesions as a potential for dose de-escalation. *Radiat Oncol*. 2018;13:24.
- Ohtakara K, Hayashi S, Hoshi H. Dose gradient analyses in Linac-based intracranial stereotactic radiosurgery using Paddick's gradient index: consideration of the optimal method for plan evaluation. *J Radiat Res*. 2011;52:592–599.
- Paddick I, Lippitz B. A simple dose gradient measurement tool to complement the conformity index. *J Neurosurg*. 2006;105:194–201.
- Hong L, Shankar V, Shen J, et al. Spine stereotactic body radiation therapy plans: achieving dose coverage, conformity, and dose falloff. *Med Dosim*. 2015;40:181–185.
- Goldbaum D, Hurley J, Hamilton R. A simple knowledge-based tool for stereotactic radiosurgery pre-planning. *J Appl Clin Med Phys*. 2019;20:97–108.
- Hurkmans C, Cuijpers J, Lagerwaard F, et al. Recommendations for implementing stereotactic radiotherapy in peripheral state IA non-small cell lung cancer: report from the quality assurance working party of the randomized phase III ROSEL study. *Radiat Oncol*. 2009;4:1.
- Weksberg D, Palmer M, Vu K, et al. Generalized class solutions for treatment planning of spinal stereotactic body radiation therapy. *Int J Radiat Oncol Biol Phys*. 2012;84:847–853.